

See discussions, stats, and author profiles for this publication at: <https://www.researchgate.net/publication/305847922>

Extended mild-slope equation for surface waves interacting with a vertically sheared current

Article · October 2016

DOI: 10.1016/j.coastaleng.2016.06.003

READS

4

4 authors, including:



[Julien Touboul](#)

Université de Toulon

50 PUBLICATIONS 210 CITATIONS

[SEE PROFILE](#)

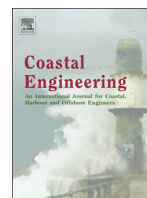


[K.A. Belibassakis](#)

National Technical University of Athens

121 PUBLICATIONS 1,102 CITATIONS

[SEE PROFILE](#)



Extended mild-slope equation for surface waves interacting with a vertically sheared current



J. Touboul^{a,b,*}, J. Charland^{a,b,c}, V. Rey^{a,b}, K. Belibassakis^d

^a Université de Toulon, CNRS / INSU, IRD, MIO, UM 110, 83041 Toulon, Cedex 9, France

^b Aix-Marseille Université, CNRS / INSU, IRD, MIO, UM 110, 13284 Marseille, France

^c DGA, CNRS Délégation Normandie, France

^d National Technical University of Athens, School of Naval Architecture & Marine Engineering, Athens, Greece

ARTICLE INFO

Article history:

Received 19 June 2015

Revised in revised form 24 May 2016

Accepted 11 June 2016

Available online xxxx

Keywords:

Extended mild-slope equation

Water waves

Current interaction

Bottom interaction

Constant vorticity

ABSTRACT

Propagation of water waves in coastal zones is mainly affected by the influence of currents and bathymetry variations. Models describing wave propagation in coastal zones are often based on the numerical solution of the Mild Slope equation (Kirby, 1984). In this work, an extension of this equation is derived, taking into account the linear variation of the current with depth, which results in a constant horizontal vorticity, slowly varying horizontally, within the background current field. The present approach is based on the asymptotic expansion of the depth-integrated Lagrangian, assuming the linear variation of the background current with depth. With the aid of selected examples the role of this horizontal vorticity, associated with the assumed background current velocity profile, is then illustrated and emphasized, demonstrating its effect on the propagation of water waves in coastal areas.

© 2016 Published by Elsevier B.V.

1. Introduction

In coastal areas, steep bathymetries and strong currents are often observed. Among several causes, the presence of cliffs, rocky beds, or human structures may cause strong variations of the sea bed, while oceanic circulation, tides, wind action or wave breaking can be responsible for the generation of strong currents. Furthermore, given these generation processes, the currents are often observed to vary with depth, and vorticity contained within strong tidal currents (see, e.g., Soulsby, 1990, Section 3) or in wind driven currents (see, e.g., Jonsson, 1990, Section 6) could be important and should be taken into account in modelling the propagation of water waves. This is especially true in applications in nearshore and coastal regions (see, e.g., Thomas and Klopman, 1997; Massel, 1993, Ch.8), where additional factors due to bathymetry variations and flow termination at the shoreline contribute into increasing complexity of the current flow. In the latter case, wave–seabed, wave–current and wave–vorticity interactions constitute three kinds of inhomogeneities with significant impact on water wave dynamics. As a first approximation, under the assumption of slow horizontal variations and waves of small amplitude, the effect of the current vorticity due to vertical shear could be separated from the one associated with horizontal variation of the mean (depth averaged) current flow.

For the purpose of modelling wave–bottom interactions, a major step was due to Berkhoff (1976), who derived a linear, elliptic equation taking into account the combined effects of reflection, diffraction and refraction of water waves on varying bathymetries. In his approach, he used a perturbative development, assuming slowly varying bottoms. Since these pioneer works, several authors extended this equation to take steep bathymetry effects into account. Indeed, in this configuration, local modes are known to play a significant role on the propagation of water waves (Rey, 1992; Mei, 1994). This role was especially emphasized by Kirby and Dalrymple (1983), who explained tunnel effect through the presence of these modes. In the absence of currents, Massel (1993), and later on, Chamberlain and Porter (1995) extended Berkhoff's equation to include the effect of local modes. More recently, Athanassoulis and Belibassakis (1999) improved the equation by including a “bottom mode” in the local mode decomposition.

Modelling the interaction of waves and currents is also of primary matter to describe efficiently water wave propagation in coastal areas. The influence of currents on wave dynamics is known to be significant. For instance, the formation of giant waves in the Agulhas current, which flows along the south–east coast of Africa, was explained through wave current interactions (Smith, 1976; Lavrenov and Porubov, 2006). Several theoretical works initially studied the influence of wave current interactions (see e.g. Longuet-Higgins and Stewart, 1961), neglecting the influence of bathymetry in the process. Complete reviews can be found in Whitham (1974); Peregrine (1976) and Jonsson (1990). In the framework of coastal wave propagation modelling, Booij (1981)

* Corresponding author at: Université de Toulon, CNRS / INSU, IRD, MIO, UM 110, 83041 Toulon, Cedex 9, France.

E-mail address: julien.touboul@univ-tln.fr (J. Touboul).

and Liu (1983) were the first authors to extend Berkhoff's equation, allowing to take wave – current interactions into account in the presence of arbitrary bathymetric variations. In these formulations, the current was assumed to vary horizontally, presenting a uniform vertical structure. However, both of these equations neglected some terms describing the horizontal variation of the currents. A full formulation of the problem was finally introduced by Kirby (1984). Based on a variational approach, and a linearized description of the lagrangian of the problem, this author derived an elliptic equation describing water waves interacting with a slowly varying bottom, and currents vertically uniform, but varying horizontally. This equation is known as the “mild-slope” equation, commonly used in coastal wave propagation models. More recently, the formulation obtained by Kirby (1984) was extended to recent versions of Berkhoff's equation, allowing to model wave interaction with abrupt bathymetries and varying currents (Belibassakis, 2007).

Another physical process, however, the wave–vorticity interaction, is known to have a significant influence on water waves dynamics when vorticity is present in the background field. This is an important aspect especially in the case of slowly varying environmental currents, where the vertical structure of the boundary layer in the nearshore and coastal region could occupy the entire depth, as in the case of tidal currents; see, e.g., Soulsby (1990) and Thomas and Klopman (1997). Various studies concerning the vertical structure of current in the coastal zone including measured data (e.g. Greenwood and Osborne, 1990; Putrevu and Svendsen, 1993; Haas and Svendsen, 2002) show that the flow is vortical, signifying the importance of modelling the effects of depth-dependent current on wave propagation in coastal regions. Furthermore, recent experiments studied the dynamics of water waves propagating in the presence of strongly sheared currents, and demonstrated the inability of the Mild Slope equation to represent water waves dynamics in the presence of background vorticity (Rey et al., 2012; Rey et al., 2014). However, few studies investigated the influence of sheared currents on water waves propagation, and no model, to our knowledge, allows to represent the dynamics of water waves in two dimensions of propagation, in the presence of current, vorticity, and bathymetric variations, all of them presenting slow variations with respect to the wave scales.

Pioneer works describing the interaction of water waves with vertically sheared currents are due to Dalrymple (1974) and Stewart and Joy (1974), who considered shearing as a small perturbation of uniform currents. Several authors succeeded in describing the dispersion relation of water waves propagating in the presence of various vorticity in linear (Skop, 1987a, 1987b; Kirby and Chen, 1989) or nonlinear theory (Shrira (1993); Liu et al. (2014)). For depth varying currents, however, the derivation of variational formulations is not straightforward, since the flow is not irrotational. This explains the lack of models describing the evolution of water waves propagating in the presence of vorticity. In the specific case of linearly sheared currents, however, several authors overcame this difficulty. Among them, Jonsson et al. (1978) studied wave action conservation in the framework of one dimensional wave propagation over varying bathymetry. Later on, Simmen and Saffman (1985) and Teles Da Silva and Peregrine (1988) derived a variational formulation of the problem, and used it to obtain an exact solution for steady water waves numerically. However, all these cases are limited to two dimensional flows, which allow to describe water waves propagating in one dimension.

The purpose of this work is twofold. First, a method is developed in order to extend the mild-slope equation for the propagation of water waves over slowly varying bathymetries, in the presence of spatially varying sheared currents presenting a linear distribution in the vertical direction. The lagrangian introduced by Simmen (1984) is linearized following a method similar to the one used by Kirby (1984). Once the equation derived, we solve numerically both the one and the two dimensional versions of this equation. The purpose of this second part is to emphasize the strong influence of vorticity, slowly varying horizontally, on the waves dynamics.

2. Linear water waves in the presence of constant vorticity

2.1. Description of the current structure, bathymetry and wave fields

We consider the scattering of water waves by slowly variable bathymetry, in the presence of a vertically sheared current, which is slowly varying in the horizontal directions. A Cartesian coordinate system (x, z) is used with origin at some point on the undisturbed free surface, and the vertical z -axis pointing upwards. The seabed surface is defined by $z = -h_0(\delta x)$ and the current is assumed to be of the form

$$\mathbf{U}(\mathbf{x}, z) = \mathbf{U}_0(\delta \mathbf{x}) + \mathbf{S}(\delta \mathbf{x})z, \quad (1)$$

where $\mathbf{U}_0 = (u_x, u_y)$, $\mathbf{S} = (s_x, s_y)$, and where δ is a small parameter. The vorticity $\boldsymbol{\Omega} = \nabla \times \mathbf{U}$ contained in the current has components

$$\boldsymbol{\Omega} = (-s_y, s_x, \Omega_z), \quad \text{where} \quad \Omega_z = \left(\frac{\partial s_y}{\partial x} - \frac{\partial s_x}{\partial y} \right) z + \left(\frac{\partial u_y}{\partial x} - \frac{\partial u_x}{\partial y} \right). \quad (2)$$

On the basis of the assumption (1), the vertical component of the vorticity is significantly smaller than the horizontal ones, and will be considered zero in the present work. Thus, the surface current and shear fields, respectively, satisfy

$$\nabla \times \mathbf{U}_0 = 0, \quad \nabla \times \mathbf{S} = 0, \quad \text{and thus} \quad \boldsymbol{\Omega} = (-s_y, s_x, 0). \quad (3)$$

When modelling water waves in the presence of vorticity, a major question concerns the description of the vorticity inherent to the wave field. The question of irrotationality of the flow due to water waves, and the subsequent representation by means of potential theory, has to be considered with caution. In the specific case of constant vorticity, however, this question might be addressed rigorously. In the present study, we might follow Simmen (1984) and Simmen and Saffman (1985), and look for wavy solutions in the form

$$\mathbf{u}(\mathbf{x}, z, t) - \mathbf{U}(\mathbf{x}, z) = \nabla \Phi(\mathbf{x}, z, t), \quad (4)$$

where \mathbf{u} corresponds to the total flow, and Φ is a potential solution describing a perturbation of the mean sheared flow \mathbf{U} , which satisfies the Laplace equation. This assumption implies no vorticity within the wave field, which, by itself, needs a proper justification. A mathematical demonstration of this postulate can be found in Nwogu (2009), where the vorticity conservation equation of the total velocity field for water waves propagating on a current varying vertically with an arbitrary profile is studied. The vorticity of the perturbative field (the wave field), was found to be transported by the waves, except for a single source-sink term involving the second derivative with respect to z of the background sheared current. Thus, water waves initially involving no vorticity will keep propagating with an irrotational motion of the fluid, as long as the current variations with depth remain linear. This property of the motion will be tested by comparisons with experimental results available in the literature in Section 2.3.

2.2. Integration of Euler equations in the presence of vorticity

If integrating Euler equations in a scalar description is of current knowledge while considering irrotational flow, it is not straightforward in the framework of the problem at hand. When considering flow fields involving two non-zero components of the vorticity, Stepanyants and Yakubovich (2011) recently introduced a method allowing to find a scalar description of the field. We follow similar approach in order to integrate Euler equations. The latter, written both for the background current field and for the total field including the wave disturbance and

subtracting by parts reduce to the following form

$$\nabla \left(\frac{\partial \Phi}{\partial t} + (\mathbf{U}_0 + \mathbf{S}z) \cdot \nabla \Phi + \frac{(\nabla \Phi)^2}{2} + gz \right) + \boldsymbol{\Omega} \times \nabla \Phi = \nabla \left(-\frac{p}{\rho} \right), \quad (5)$$

where p stands for the disturbance pressure. For sake of clarity, and given the specific structure of the flow, we might restrict the operator ∇ to the horizontal components of the gradient, and write $\nabla = (\nabla_h, \partial/\partial z)$. Thus, the above equation might be rewritten

$$\begin{aligned} \nabla_h \left(\frac{\partial \Phi}{\partial t} + (\mathbf{U}_0 + \mathbf{S}z) \cdot \nabla_h \Phi + \frac{(\nabla_h \Phi)^2}{2} + \frac{1}{2} \left(\frac{\partial \Phi}{\partial z} \right)^2 + gz \right) + \frac{\partial \Phi}{\partial z} \mathbf{S} \\ = \nabla_h \left(-\frac{p}{\rho} \right), \end{aligned} \quad (6a)$$

$$\begin{aligned} \frac{\partial}{\partial z} \left(\frac{\partial \Phi}{\partial t} + (\mathbf{U}_0 + \mathbf{S}z) \cdot \nabla_h \Phi + \frac{(\nabla_h \Phi)^2}{2} + \frac{1}{2} \left(\frac{\partial \Phi}{\partial z} \right)^2 + gz \right) - \mathbf{S} \cdot \nabla_h \Phi \\ = -\frac{1}{\rho} \frac{\partial p}{\partial z}. \end{aligned} \quad (6b)$$

The difficulty lies on integrating the last terms of the left hand side of the above equations. To do so, we might introduce a vector stream function, as it was suggested by Toledo and Agnon (2011), and thus

$$\Psi(\mathbf{x}, z, t) = \left(\Psi^{(1)}(\mathbf{x}, z, t), \Psi^{(2)}(\mathbf{x}, z, t) \right) = \int_{-h}^z \nabla_h \Phi d\xi. \quad (7)$$

In this definition, h corresponds to the local water depth, i.e. $h = h_0 - \eta_0$, where h_0 is the depth of the bathymetry, and η_0 the deviation of the surface due to the presence of the current. This vector stream function fulfils the relations

$$\nabla_h \cdot \Psi = -\frac{\partial \Phi}{\partial z} \quad \text{and} \quad \frac{\partial \Psi}{\partial z} = \nabla_h \Phi. \quad (8)$$

Thus, the last term of left hand side of Eqs. (6a) and (6b) respectively rewrites $-\mathbf{S}(\nabla_h \cdot \Psi)$ and $\mathbf{S} \cdot \partial \Psi / \partial z$.

Since \mathbf{S} is not a function of z , transformation of the second term is straightforward, and $\mathbf{S} \cdot \partial \Psi / \partial z = \partial(\mathbf{S} \cdot \Psi) / \partial z$. Transformation of the first term, however, needs more algebra. We might take advantage of the two classical relations of vectorial analysis, expressing and the term $\mathbf{S}(\nabla \cdot \Psi)$ in the following form

$$\mathbf{S}(\nabla \cdot \Psi) = \nabla(\mathbf{S} \cdot \Psi) - (\mathbf{S} \times \nabla) \times \Psi - (\nabla \cdot \mathbf{S})\Psi - (\Psi \times \nabla) \times \mathbf{S}. \quad (9)$$

If restricted to the two horizontal components, this relation becomes

$$\mathbf{S}(\nabla_h \cdot \Psi) = \nabla_h(\mathbf{S} \cdot \Psi) - (\mathbf{S} \times \nabla_h) \times \Psi - (\nabla_h \cdot \mathbf{S})\Psi - (\Psi \times \nabla_h) \times \mathbf{S}. \quad (10)$$

Following Stepanyants and Yakubovich (2011), we can write the equation of conservation of vorticity. Since the vertical component of the vorticity is nil, its conservation, projected on the z axis, writes here

$$[(\nabla(z) \times \mathbf{S}) \cdot \nabla](\nabla \cdot \Psi) = 0. \quad (11)$$

If Ψ is described as a wavy perturbation of wavenumber \mathbf{k} , it results that $\nabla \cdot \Psi = i\mathbf{k} \cdot \Psi$, and the equality (11) implies that vectors \mathbf{k} and \mathbf{S} are necessarily collinear. Thus, water waves propagating in the presence of constant vorticity have to be two-dimensional, and to propagate collinearly with vector \mathbf{S} . This confirms the result initially derived by Constantin (2011).

Given the definition of Ψ , we can note that $\partial \Psi^{(1)} / \partial y = \partial \Psi^{(2)} / \partial x$. Using these two remarks allows to demonstrate the relation

$$(\mathbf{S} \times \nabla_h) \times \Psi = |\mathbf{S}| \mathcal{O}(\delta). \quad (12)$$

Finally, it comes now clear that

$$-\mathbf{S}(\nabla_h \cdot \Psi) = -\nabla_h(\mathbf{S} \cdot \Psi) + (|\mathbf{U}_0| + |\mathbf{S}|) \mathcal{O}(\delta), \quad (13a)$$

$$\text{and} \quad -\mathbf{S} \cdot \frac{\partial \Psi}{\partial z} = -\frac{\partial(\mathbf{S} \cdot \Psi)}{\partial z}. \quad (13b)$$

The Euler Eqs. (6a) and (6b) can now be integrated, and dropping the $\mathcal{O}(\delta)$ terms, we finally obtain the pressure field, given by

$$-\frac{p}{\rho} = \frac{\partial \Phi}{\partial t} + (\mathbf{S}z + \mathbf{U}_0) \cdot \nabla \Phi + \frac{(\nabla \Phi)^2}{2} + \frac{1}{2} \left(\frac{\partial \Phi}{\partial z} \right)^2 - \mathbf{S} \cdot \Psi + gz + |\mathbf{S}| \mathcal{O}(\delta). \quad (14)$$

In the above equation, and in the following, the subscript of the operator ∇_h will be dropped, since no confusion can arise anymore.

2.3. Linear solution of the wave field

As it is classically done (see e.g. Dean and Dalrymple, 1991), we might introduce non-dimensional variables, based on characteristic scales related to the waves. Thus, if \mathbf{k} denotes the wave vector, $k = |\mathbf{k}|$ the related wavenumber, and a the waves amplitude, we may consider non dimensional variables $\hat{\mathbf{x}} = k\mathbf{x}$, $\hat{z} = kz$, $\hat{t} = \sqrt{gk}t$. The angular frequency of the waves is now given by $\hat{\omega} = \omega / \sqrt{gk}$. Given these new variables, the fields describing water waves, namely the elevation η , velocity potential Φ , stream function Ψ and pressure p , now write

$$\hat{\eta} = \frac{\eta}{a}, \quad \hat{\Phi} = \frac{k}{a\sqrt{gk}}\Phi, \quad \hat{\Psi} = \frac{k}{a\sqrt{gk}}\Psi \quad \text{and} \quad \hat{p} = \frac{k}{\rho g}p. \quad (15)$$

Furthermore, the current field should also be written in a non dimensional form, so that

$$\hat{\mathbf{U}}_0 = \sqrt{\frac{k}{g}}\mathbf{U}_0 \quad \text{and} \quad \hat{\mathbf{S}} = \frac{\mathbf{S}}{\sqrt{gk}}. \quad (16)$$

When written in a non dimensional formulation, the hypothesis of slow variations of the fields might rewrite $|\nabla_h \Phi| = \mathcal{O}(\delta)$, $|\nabla \cdot \hat{\mathbf{U}}_0| = \mathcal{O}(\delta)$ and $|\nabla \cdot \hat{\mathbf{S}}| = \mathcal{O}(\delta)$. Then, if introducing this formalism within the Bernoulli Eq. (14), the latter becomes

$$\begin{aligned} -\hat{p} = \hat{z} + \varepsilon \left(\frac{\partial \hat{\Phi}}{\partial \hat{t}} + (\hat{\mathbf{S}}\hat{z} + \hat{\mathbf{U}}_0) \cdot \nabla \hat{\Phi} - \hat{\mathbf{S}} \cdot \hat{\Psi} \right) \\ + \frac{\varepsilon^2}{2} \left((\nabla \hat{\Phi})^2 + \left(\frac{\partial \hat{\Phi}}{\partial \hat{z}} \right)^2 \right) + \mathcal{O}(\delta). \end{aligned} \quad (17)$$

Since Φ can be understood as a perturbation of the mean flow, we introduce the perturbative approximation

$$\begin{aligned} \hat{\Phi}(\mathbf{x}, z, t) = \phi(\mathbf{x}, z, t) + \mathcal{O}(\varepsilon), \\ \Psi(\mathbf{x}, z, t) = \psi(\mathbf{x}, z, t) + \mathcal{O}(\varepsilon), \\ \eta_T(\mathbf{x}, t) = \eta_0(\mathbf{x}) + \eta(\mathbf{x}, t) + \mathcal{O}(\varepsilon), \end{aligned} \quad (18)$$

where ϕ , ψ , η_0 and η are nondimensional quantities of order $\mathcal{O}(1)$. In Eq. (18), η_T refers to the total deviation of the free surface from its rest position. Namely, η_0 is the deviation due to the presence of the current, and η refers to the influence of waves. Finally, ε is a small parameter, the wave steepness, defined as $\varepsilon = ak$, a being the wave amplitude and $k =$

$|\mathbf{k}|$ the wavenumber of the perturbation. For sake of readability, every hat will be discarded in the following.

If neglecting completely any horizontal variations, we derived a set of equations which might be satisfied by water waves in the presence of constant vorticity. In two horizontal dimensions of propagation, the system to be satisfied writes

$$\begin{aligned} \varepsilon \Delta \Phi &= 0 && \text{for } -h \leq z \leq \eta, \\ \varepsilon \left(\frac{\partial \Phi}{\partial t} + \mathbf{U}_0 \cdot \nabla \Phi - \mathbf{S} \cdot \Psi + \eta \right) + \varepsilon^2 \left(\frac{(\nabla \Phi)^2}{2} + \frac{1}{2} \left(\frac{\partial \Phi}{\partial z} \right)^2 + \eta \mathbf{S} \cdot \nabla \Phi \right) &= 0 && \text{on } z = \eta, \\ \varepsilon \left(\frac{\partial \eta}{\partial t} + \mathbf{U}_0 \cdot \nabla \eta - \frac{\partial \Phi}{\partial z} \right) + \varepsilon^2 \eta \mathbf{S} \cdot \nabla \eta &= 0 && \text{on } z = \eta, \\ \text{and } \varepsilon \frac{\partial \Phi}{\partial z} &= 0 && \text{on } z = -h. \end{aligned} \quad (19)$$

Thus, the system (19) can be further linearized with respect to the wave steepness, and becomes, after dropping every term of order $\mathcal{O}(\varepsilon^2)$, and coming back to dimensional variables,

$$\begin{aligned} \Delta \phi &= 0 && \text{for } -h \leq z \leq \eta, \\ \frac{\partial \phi}{\partial t} + \mathbf{U}_0 \cdot \nabla \phi - \mathbf{S} \cdot \psi + g \eta &= 0 && \text{on } z = \eta, \\ \frac{\partial \eta}{\partial t} + \mathbf{U}_0 \cdot \nabla \eta &= \frac{\partial \phi}{\partial z} && \text{on } z = \eta, \\ \text{and } \frac{\partial \phi}{\partial z} &= 0 && \text{on } z = -h. \end{aligned} \quad (20)$$

Solutions of this system can be found by searching the velocity potential in the form of a wavy perturbation, $\phi(\mathbf{x}, z, t) = \phi_0 f(z) e^{i(\mathbf{k} \cdot \mathbf{x} - \omega t)}$. From this assumption, it follows that $f(z) = \cosh(k(z+h))/\cosh(kh)$, where $k = |\mathbf{k}|$, and we obtain the expressions

$$\begin{aligned} \phi(\mathbf{x}, z, t) &= \phi_0 \frac{\cosh(k(z+h))}{\cosh(kh)} e^{i(\mathbf{k} \cdot \mathbf{x} - \omega t)} \\ \eta(\mathbf{x}, t) &= a e^{i(\mathbf{k} \cdot \mathbf{x} - \omega t)} \\ \psi(\mathbf{x}, z, t) &= i \mathbf{k} \phi_0 \frac{\sinh(k(z+h))}{k \cosh(kh)} e^{i(\mathbf{k} \cdot \mathbf{x} - \omega t)} \end{aligned} \quad (21)$$

Furthermore, the dispersion relation is found to be

$$(\omega - \mathbf{k} \cdot (\mathbf{U}_0 - (\tanh(kh)/2k)\mathbf{S}))^2 - (\mathbf{k} \cdot (\tanh(kh)/2k)\mathbf{S})^2 = gk \tanh(kh), \quad (22)$$

confirming the pioneer results of [Thompson \(1949\)](#) and [Kirby and Chen \(1989\)](#). The physical interpretation of this relation, however, is not straightforward, and deserve further consideration.

In the framework of water waves propagating on a vertically sheared current, many studies intended to obtain an analogy with the case of water waves propagating over a vertically uniform current \mathbf{U}_{eq} . Within this approach, the question of the definition of the equivalent uniform current arises. The problem is to define a value of this current correctly chosen to reproduce the dynamics of water waves. Thus, an equivalent depth d_e might naturally be introduced. Indeed, this depth will be defined as the depth where the sheared current equals the equivalent uniform current ($\mathbf{U}_0 - d_e \mathbf{S} = \mathbf{U}_{eq}$). Among others, [Stewart and Joy \(1974\)](#) introduced a value of d_e equal to $\lambda/4\pi$, λ referring to the local wavelength.

However, the idea of an equivalent uniform current might be questioned. Indeed, the experimental results obtained by [Thomas \(1990\)](#), and confirmed later by [Swan et al. \(2001\)](#), shed some light about the internal flow beneath surface waves propagating over a vertically sheared current of arbitrary profile. While considering two dimensional waves propagating over a flat bottom, these authors observed some local inversions of the orbital velocities. This behaviour can

certainly not be described through the superposition of a constant current, whatever its value, and irrotational waves. In the specific case of a constant vorticity, [Wahlen \(2009\)](#) and [Constantin and Varvaruca \(2011\)](#) demonstrated theoretically that critical layers, or stagnation points, might appear for specific values of the mean flow vorticity.

In the latter case, these questions have an echo in the dispersion relation. Indeed, while considering water waves propagating over linearly sheared currents, the exact linear dispersion relation is given by relation (22). Under the hypothesis of weak shearing, namely $|(\tanh(kh)/k)\mathbf{S}|/|\mathbf{U}_0| \ll 1$, the second term in the left hand side of this equation vanishes, which demonstrates the validity of the approach of [Stewart and Joy \(1974\)](#). Discarding this term will directly allow to identify the equivalent depth $d_e = \tanh(kh)/2k$, and the equivalent current $\mathbf{U}_1 = \mathbf{U}(z = -d_e) = \mathbf{U}_0 - d_e \mathbf{S}$. Under this assumption, the frequency, $\sigma^2 = gk \tanh(kh)$, corresponds to the intrinsic frequency σ_1 for waves transported at the velocity \mathbf{U}_1 ($\sigma_1 = \omega - \mathbf{k} \cdot \mathbf{U}_1$). It is interesting to notice that this equivalent depth d_e admits the asymptotic value $\lambda/4\pi$ when $kh \rightarrow \infty$, confirming the results by [Stewart and Joy \(1974\)](#). However, while considering the shallow water limit $kh \rightarrow 0$, the asymptotic value of the equivalent depth becomes $h/2$, and \mathbf{U}_1 is now the mean value of the current. It also has to be mentioned that this depth corresponds to the ‘‘wave depth’’ introduced by [Teles Da Silva and Peregrine \(1988\)](#).

In the general case, however, the second term in the left hand side of Eq. (22) cannot be neglected, and the above approximation does not hold anymore. This relation might however be rewritten

$$(\omega - \mathbf{k} \cdot (\mathbf{U}_0 - 2d_e \mathbf{S}))(\omega - \mathbf{k} \cdot \mathbf{U}_0) = gk \tanh(kh). \quad (23)$$

Thus, the intrinsic frequency $\sigma^2 = gk \tanh(kh)$ cannot be understood anymore as simple translation at the velocity $\mathbf{U}(-d_e)$. Indeed, within this approach, we have to introduce the velocities and the angular frequencies

$$\begin{aligned} \mathbf{U}_0 &= \mathbf{U}(0) && \text{and } \sigma_0 = \omega - \mathbf{k} \cdot \mathbf{U}_0, \\ \mathbf{U}_1 &= \mathbf{U}(-d_e) && \text{and } \sigma_1 = \omega - \mathbf{k} \cdot \mathbf{U}_1, \\ \mathbf{U}_2 &= \mathbf{U}(-2d_e) && \text{and } \sigma_2 = \omega - \mathbf{k} \cdot \mathbf{U}_2. \end{aligned} \quad (24)$$

Thus, the dispersion relation reduces to $\sigma^2 = \sigma_0 \sigma_2$, and intrinsic frequency σ has to be understood as the geometric mean of the frequencies σ_0 and σ_2 . In other terms, a single equivalent velocity \mathbf{U}_{eq} cannot be defined, but an intrinsic equivalent frequency can be obtained by considering the Doppler shift due to the two velocities \mathbf{U}_0 and \mathbf{U}_2 .

2.4. Velocity profile in the presence of vorticity

As discussed in [Section 2.1](#), the present model is based on the assumption that, for waves propagating in a vertically sheared current with constant vorticity, the wave field could be approximately treated as irrotational; see, also [Thomas and Klopman \(1997\)](#), Section 3.1.1). Secondly, one-way coupling between the current and water waves has been assumed, and the effect of water waves on the current profile is neglected. In this section, in order to test the above assumptions, comparisons are shown between predictions by present model, experimental data and results from the model derived by [Son and Lynett \(2014\)](#), which takes the two-way wave current coupling into account.

The case of opposing waves on a vertically sheared current was studied experimentally by [Swan \(1990\)](#), where the influence of strong vorticity on the behaviour of water waves, was analyzed experimentally. Indeed, this author performed a series of measurements describing two dimensional water waves, in the vertical plane, propagating in opposing strongly sheared currents. Among other results, in the latter work, the evolution of horizontal component of the wave velocity is presented as a function of depth for various conditions. Within the present approach, if the wave induced motion is described by means of potential theory (see Eq. (21)), the horizontal velocities are easily obtained by

differentiating with respect to \mathbf{x} , and it comes

$$U_{waves}(z, t) = \frac{agk\sigma_0}{\sigma^2} \frac{\cosh(k(z+h))}{\cosh(kh)} e^{i(kx-\omega t)}, \quad (25)$$

where a is the amplitude of the free surface elevation and k is the solution of the modified dispersion relation in the presence of linearly sheared current, Eq. (23). We remark here that in constant depth and horizontally constant surface current U_0 and shear S , the above result is also an exact solution of the extended mild slope equation for surface waves interacting with vertically sheared current that will be presented and discussed in detail in the next section. A comparison between the experimental data (green circles) and the predictions obtained by means of linear potential theory is shown in Fig. 1, for various current, vorticity and wave conditions.

Another basic assumption of the present model concerning the one-way coupling between the current and water waves could also be questioned. Indeed, the influence of water waves on the background current is not considered here. In a recent work by Son and Lynett (2014), a numerical model based on Boussinesq-type equations is derived, taking into account the full coupling of nonlinear water waves with a sheared current. Numerical results from the latter work are presented in Fig. 2 together with the experimental data by Swan (1990). For sake of comparison, results provided by the present model are also plotted in this figure, showing quite good agreement with the measured data, especially as concerns the horizontal velocities at various depths below the free surface. This agreement clearly indicates that the two-way coupling does not have a significant influence on water waves dynamics. The largest discrepancies between the linear potential theory and the experimental results of Swan (1990) appear on Fig. 2(a), and concern the free surface elevation. In this figure, we clearly observe the effect of wave nonlinearity, which manifests in the vicinity of the free surface. However, if considering the orbital velocities, these comparisons with experimental data by Swan (1990) and nonlinear numerical model by Son and Lynett (2014) validate the potential linear approach, and more specifically the vertical variation of the velocity

potential as the function $f(z) = \cosh(k(z+h))/\cosh(kh)$, to be reasonably accurate.

3. Derivation of the extended mild slope equation

In this section, we use a variational formulation to derive an evolution equation for water wave propagation when slow variations of the bathymetry, surface current and vorticity are considered. The expression of the lagrangian that should be considered in the framework of flow with vorticity, however, should be introduced carefully. Indeed, the conservative lagrangian in vortical flows was initially introduced by Bateman (1929), using Clebsch's potential formulation. Luke (1967) extended this result to flows with free surface. Then, Seliger and Whitham (1968) demonstrated that the term used in Bateman (1929) and Luke (1967) did correspond to the vertical integration of the pressure term. Indeed, the quantity \mathcal{L} defined by

$$\mathcal{L} = \int_{-h}^{\eta} -p dz. \quad (26)$$

should be conservative for flows with vorticity, as it was stated by Longuet-Higgins (1983). Given the assumptions formulated above, the lagrangian \mathcal{L} can be rewritten

$$\mathcal{L}(\phi, \eta) = \int_{-h}^{\eta} \left\{ z + \varepsilon \left(\frac{\partial \phi}{\partial t} + (\mathbf{S}z + \mathbf{U}_0) \cdot \nabla \phi - \mathbf{S} \cdot \boldsymbol{\psi} \right) + \varepsilon^2 \left(\frac{(\nabla \phi)^2}{2} + \frac{1}{2} \left(\frac{\partial \phi}{\partial z} \right)^2 \right) \right\} dz + \mathcal{O}(\delta). \quad (27)$$

The above equation can be put in the form

$$\mathcal{L}(\phi, \eta) = \mathcal{L}_1 + \varepsilon^2 \left\{ \frac{\eta^2}{2} + \eta \left(\frac{\partial \phi}{\partial t} + \mathbf{U}_0 \cdot \nabla \phi - \mathbf{S} \cdot \boldsymbol{\psi} \right)_{z=0} + \frac{1}{2} \int_{-h}^0 \left((\nabla \phi)^2 + \left(\frac{\partial \phi}{\partial z} \right)^2 \right) dz \right\} + \mathcal{O}(\varepsilon^3, \delta), \quad (28)$$

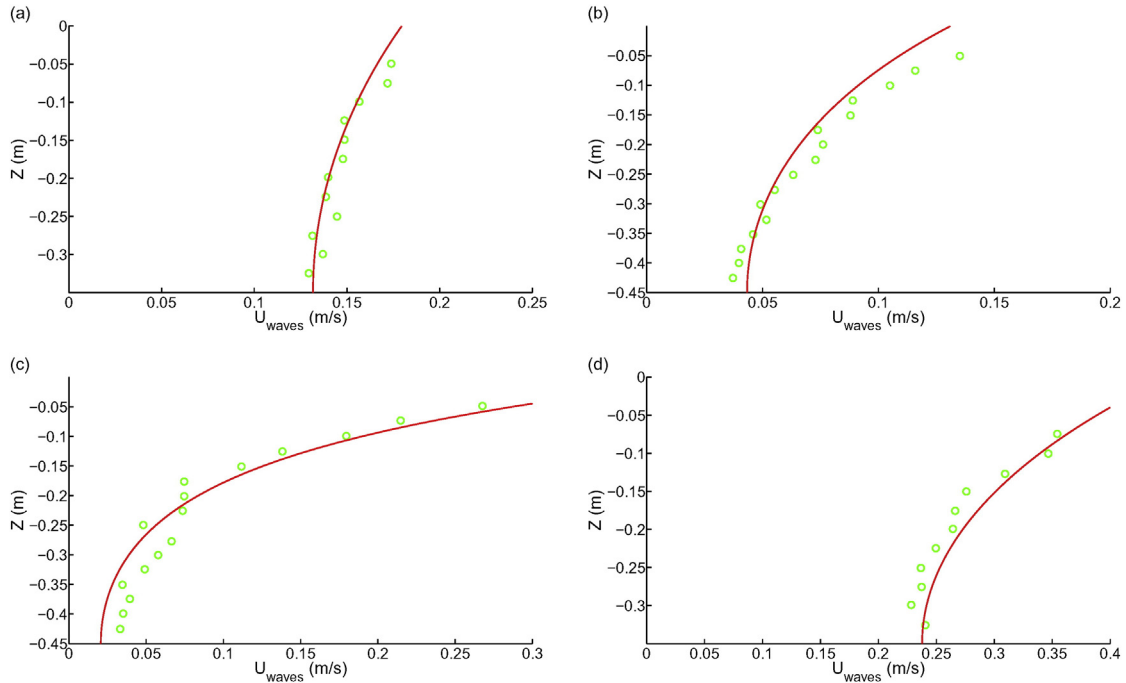


Fig. 1. Comparisons of experimental (Swan, 1990, \circ) and linear potential theory with vorticity (Eq. (25), $-$) horizontal component of the velocity induced by wave motion in various current conditions: (a): $U_0 = 0.42 \text{ m} \cdot \text{s}^{-1}$, $S_0 = 1.70 \text{ s}^{-1}$, $h = 0.35 \text{ m}$, $T = 1.418 \text{ s}$ and $a = 35.5 \text{ mm}$. (b): $U_0 = 0.44 \text{ m} \cdot \text{s}^{-1}$, $S_0 = 1.19 \text{ s}^{-1}$, $h = 0.45 \text{ m}$, $T = 0.869 \text{ s}$ and $a = 22.5 \text{ mm}$. (c): $U_0 = -0.39 \text{ m} \cdot \text{s}^{-1}$, $S_0 = -1.00 \text{ s}^{-1}$, $h = 0.45 \text{ m}$, $T = 0.998 \text{ s}$ and $a = 45.5 \text{ mm}$. (d): $U_0 = -0.50 \text{ m} \cdot \text{s}^{-1}$, $S_0 = -1.67 \text{ s}^{-1}$, $h = 0.35 \text{ m}$, $T = 1.420 \text{ s}$ and $a = 61.5 \text{ mm}$.

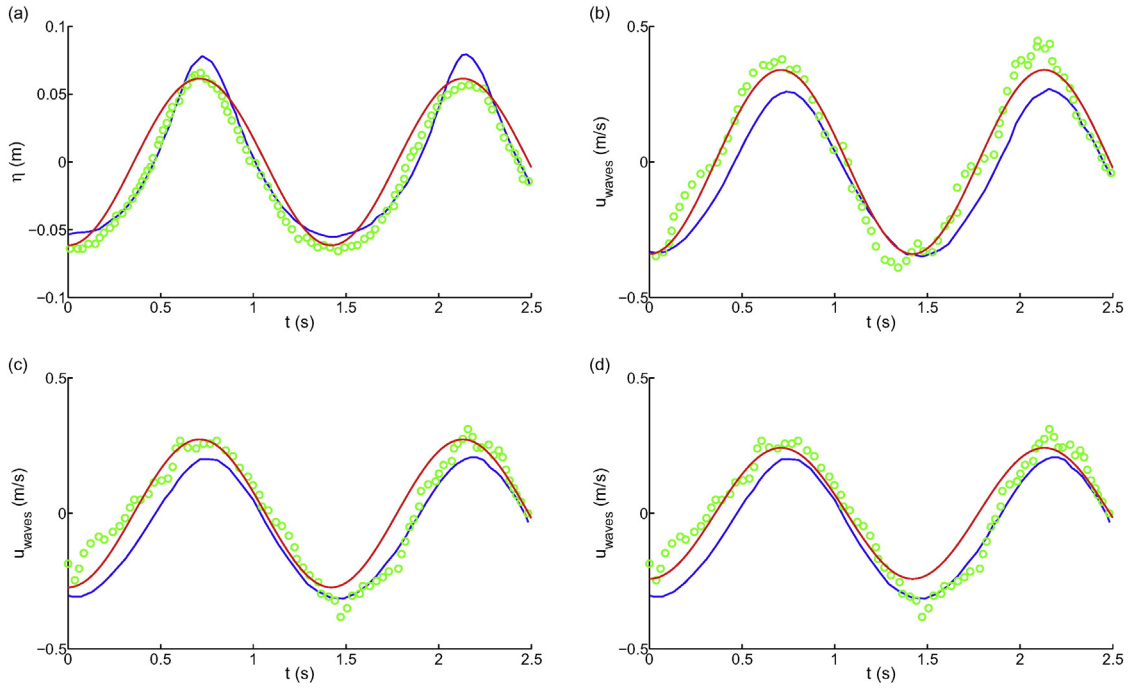


Fig. 2. Comparisons of the surface elevation (a) and horizontal component of the velocity induced by wave motion at various depth ((b): $Z = -0.1m$, (c): $Z = -0.2m$ and (d): $Z = -0.3m$) obtained by linear potential theory with vorticity (—), numerically (Son and Lynett, 2014, —) and experimentally (Swan, 1990, ○) with current conditions: $U_0 = -0.50m \cdot s^{-1}$, $S_0 = -1.67s^{-1}$, $h = 0.35m$, $T = 1.420s$ and $a = 61.5mm$.

where \mathcal{L}_1 is given by

$$\mathcal{L}_1(\phi, \eta) = -\frac{h^2}{2} + \varepsilon \int_{-h}^0 \left(\frac{\partial \phi}{\partial t} + (\mathbf{S}z + \mathbf{U}_0) \cdot \nabla \phi - \mathbf{S} \cdot \boldsymbol{\psi} \right) dz. \quad (29)$$

Following (Kirby, 1984), we might evaluate this lagrangian, based on the hypothesis of slow variations of the wave field. Indeed, keeping the perturbative approach described by Eq. (18), the velocity potential can be seek in the form

$$\phi(\mathbf{x}, z, t) = f(z)\varphi(\mathbf{x}, t) = \frac{\cosh(k(z+h))}{\cosh(kh)} \varphi(\mathbf{x}, t), \quad (30)$$

relaxing the plane wave hypothesis which was assumed in Eq. (21).

Once the vertical structure of the flow is known, we might perform the integration with respect to z , finding an expression of the lagrangian explicitly involving φ , η , and $\boldsymbol{\psi}_0$, the value of $\boldsymbol{\psi}(\mathbf{x}, z=0, t)$. Thus,

$$\mathcal{L}(\varphi, \eta) = \mathcal{L}_1 + \varepsilon^2 \left\{ \frac{\eta^2}{2} + \eta \left(\frac{\partial \varphi}{\partial t} + \mathbf{U}_0 \cdot \nabla \varphi - \mathbf{S} \cdot \boldsymbol{\psi}_0 \right) + \mathcal{L}_2 \right\} + \mathcal{O}(\varepsilon^3), \quad (31)$$

with

$$\mathcal{L}_2 = \frac{CC_g}{2} (\nabla \varphi)^2 + \frac{\sigma^2 - k^2 CC_g}{2} \varphi^2 + \frac{1}{2} \int_{-h}^0 \left(\frac{\partial f}{\partial h} \right)^2 dz (\nabla h)^2 \varphi^2 + \int_{-h}^0 f \frac{\partial f}{\partial h} dz (\nabla h) (\varphi \nabla \varphi) \quad (32)$$

In this equation, C and C_g correspond respectively to σ/k and $\partial \sigma / \partial k$, where σ is defined as $\sigma^2 = k \tanh(h)$. Assuming the last two terms of higher order $\mathcal{O}(\delta^2)$, in conjunction with the additional assumption that $\mathcal{O}(\delta) = \mathcal{O}(\varepsilon)$, these terms will be omitted.

The variational principle associated with the stationarity of Luke's functional, which is defined by the integration of the lagrangian density

given by Eq. (31), is

$$\iint_{(\mathbf{x}, t)} \frac{\partial \mathcal{L}}{\partial \varphi} \delta \varphi = 0 \quad \text{and} \quad \iint_{(\mathbf{x}, t)} \frac{\partial \mathcal{L}}{\partial \eta} \delta \eta = 0. \quad (33)$$

After substituting the above expressions, calculating the variations of the various terms, using the usual assumption that $\delta \eta$ and $\delta \varphi$ vanish at infinity, and thus, the variation $\delta \mathcal{L}_1 = 0$, we obtain using integration by parts and applying Leibnitz rule the equation system (33) reduces to

$$\frac{\partial \eta}{\partial t} + \nabla \cdot (\mathbf{U}_0 \eta) + \nabla \cdot (CC_g \nabla \varphi) - (\sigma^2 - k^2 CC_g) \varphi = 0, \quad (34)$$

and

$$\eta = - \left(\frac{\partial \varphi}{\partial t} + \mathbf{U}_0 \cdot \nabla \varphi - \mathbf{S} \cdot \boldsymbol{\psi}_0 \right), \quad (35)$$

where $\boldsymbol{\psi}_0(\mathbf{x}, 0)$ is defined by

$$\boldsymbol{\psi}_0 = \boldsymbol{\psi}(\mathbf{x}, z=0, t) = \frac{\tanh(kh)}{k} \nabla \varphi, \quad (36)$$

$\boldsymbol{\psi}$ being the function defined by Eq. (7), keeping terms up to the first order.

Returning back to dimensional variables we finally obtain the following system as a first-order approximation with respect to free surface and bottom slope

$$\frac{\partial \eta}{\partial t} + \nabla \cdot (\mathbf{U}_0 \eta) + \nabla \cdot \left(\frac{CC_g}{g} \nabla \varphi \right) - \frac{\sigma^2 - k^2 CC_g}{g} \varphi = 0, \quad (37)$$

and

$$\eta = - \frac{1}{g} \left(\frac{\partial \varphi}{\partial t} + \mathbf{U}_0 \cdot \nabla \varphi - \mathbf{S} \cdot \boldsymbol{\psi}_0 \right), \quad (38)$$

where $C = \sigma/k$, $Cg = \partial \sigma / \partial k$ and $\sigma^2 = gk \tanh(kh)$.

Keeping in mind the discussion provided in Section 2.3, we introduce two material derivatives $D/Dt = \partial/\partial t + \mathbf{U}_0 \cdot \nabla$ and $\bar{D}/\bar{D}t = \partial/\partial t + \mathbf{U}_2 \cdot \nabla$, taking into account the two velocities of transport. Then, substituting (35) and (36) into Eq. (34) leads to

$$\frac{D}{Dt} \left(\frac{\bar{D}\varphi}{\bar{D}t} \right) + (\nabla \cdot \mathbf{U}_0) \frac{\bar{D}\varphi}{\bar{D}t} - \nabla(CC_g \nabla \varphi) + (\sigma^2 - k^2 CC_g) \varphi = 0. \quad (39)$$

This equation provides an extension of the mild-slope equation, as derived by Kirby (1984), for depth varying currents. Indeed, when the variations of currents with depth are neglected ($\mathbf{S} = 0$), it is straightforward that Eq. (39) reduces to the mild-slope equation in its classic form

$$\frac{D^2 \varphi}{Dt^2} + (\nabla \cdot \mathbf{U}_0) \frac{D\varphi}{Dt} - \nabla(CC_g \nabla \varphi) + (\sigma^2 - k^2 CC_g) \varphi = 0. \quad (40)$$

Furthermore, by assuming no horizontal variations of h , \mathbf{U}_0 , nor \mathbf{S} , it is clear that Eq. (39) reduces to the linear dispersion relation (23).

4. Influence of the vorticity on the wave dynamics

The purpose of this section is to emphasize the influence, potentially strong, of the vorticity field and its horizontal variations on the propagation of water waves. This illustration is based on the numerical solution of some selected cases. In a first part, the numerical procedure for solving Eq. (39) is described. Then, results describing particular configurations of wave propagation in one and two dimensional directions are presented and commented.

4.1. Numerical solution of the extended mild slope equation

As it is classically done, Eq. (39) can be solved in the frequency domain, assuming the velocity potential to write $\varphi = \hat{\varphi} \exp(-i\omega t)$. Thus, the elliptic version of the present vertical mild shear model becomes

$$a \nabla^2 \hat{\varphi} - \nabla \cdot (\mathbf{U}_0 [\mathbf{U}_2 \cdot \nabla \hat{\varphi}]) + b \nabla \hat{\varphi} + c \hat{\varphi} = 0, \quad (41)$$

which is a second order elliptic partial derivative equation with respect to the complex wave potential $\hat{\varphi}$, and where the horizontally varying coefficients are defined as follows

$$a = CC_g, \quad (42)$$

$$b = \nabla a + i\omega(\mathbf{U}_0 + \mathbf{U}_2) \text{ and} \quad (43)$$

$$c = \omega^2 - \sigma^2 + k^2 CC_g + i\omega(\nabla \cdot \mathbf{U}_0). \quad (44)$$

The term CC_g is given by the relation

$$CC_g = \frac{g \tanh(kh)}{2k} \left(1 + \frac{2kh}{\sinh(2kh)} \right) \quad (45)$$

An important point in the case of a spatially varying environment and inhomogeneous vertical sheared current is how to define the local wavenumber appearing in the above expression. Following Belibassakis et al. (2011), in the present work this parameter is defined through the gradient of the phase

$$\mathbf{k} = \nabla \Theta, \quad \Theta = -i \ln(\varphi/|\varphi|) \quad (46)$$

of the complex wave potential. This choice introduces implicit nonlinearity to the problem and the above parameter is estimated by iterations starting from the solution corresponding to propagating waves over the environment without current. The above approach converges when the current magnitude is small compared to the phase speed of the waves.

In the examples presented in this work, 6–7 iterations are found to be sufficient to provide convergence with a relative error lower than 10^{-5} .

For the numerical solution of the problem, this equation is discretized by using a second-order, central finite difference scheme.

Two kinds of boundary conditions are considered in one dimensional propagation problems, while three kinds are considered in the two dimensional cases. In both cases, one should consider an input boundary condition located at $x = -L/2$, and an output condition located at $x = L/2$, L being the length of the numerical domain.

The input condition is obtained by imposing an incident wave potential φ_{in} , a priori known, but allowing consideration of reflected waves φ_r , as it was suggested by Panchang et al. (1991). Thus, the boundary condition at the input boundary condition reads

$$\begin{aligned} \frac{\partial \varphi}{\partial x} &= ik(\varphi_{in} - \varphi_r) \\ &= ik(2\varphi_{in} - \varphi) \quad \text{on } x = -\frac{L}{2}. \end{aligned} \quad (47)$$

In the meantime, the output boundary condition is designed to correspond to a radiation condition, allowing waves with a wave vector \mathbf{k} presenting an arbitrary, reasonably small, angle with the x axis. We implemented the boundary condition corresponding to the lower parabolic approximation (Radder, 1979; Kirby, 1989), which reads

$$\frac{\partial \varphi}{\partial x} = ik \left(\varphi + \frac{1}{2k^2} \frac{\partial^2 \varphi}{\partial y^2} \right) \quad \text{on } x = \frac{L}{2}. \quad (48)$$

Furthermore in applications to wave propagation problems in two horizontal dimensions additional conditions are used in order to model the reflection of waves from the side (lateral) boundaries ($\partial\varphi/\partial y = 0$).

4.2. One dimensional propagation

4.2.1. Wave amplification due to horizontal variations of vorticity

The first case considered here is designed to emphasize the evolution of water waves in the presence of a slowly varying vorticity field, in the absence of bathymetric variations. Thus, the numerical domain considered is one dimensional, and presents a length L . In this case, water waves of angular frequency ω are propagating in water of constant depth h , in the presence of varying current distributions $U(x, z) = U_0(x) + S(x)z$.

The spatial distributions of the fields S and U_0 are given by the relations

$$S(x) = S_0 \exp\left(-10 \frac{(x-L/2)^2}{(L/2)^2}\right). \quad (49)$$

and

$$U_0(x) = U + \frac{h}{2} S(x), \quad (50)$$

so that the flow rate is kept constant at every location x .

Results of this simulations, for $L = 20m$ and depth $h = 1m$, for wave frequency $\omega = 2\pi$ are presented in Fig. 3.

The subplot (a) compares the numerical results obtained by considering two distinct set of parameters. The blue and yellow lines correspond to water waves propagating in the presence of the current field obtained with the parameters $U = -0.2m \cdot s^{-1}$ and $S_0 = 0s^{-1}$. Given the definitions of the current (49) and (50), this current is constant, so that $U(x, z) = U$. The blue line is the corresponding elevation, while the yellow one corresponds to the related envelope. As expected, the envelope remains constant all along the numerical tank.

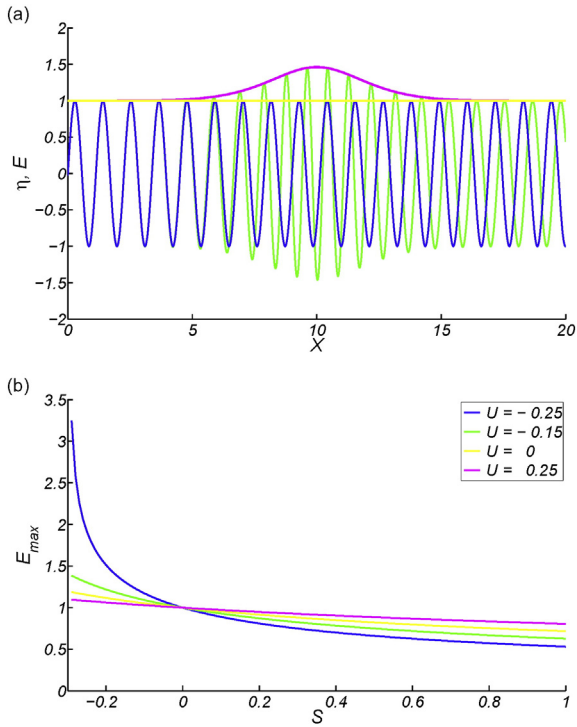


Fig. 3. (a): Comparison of the spatial evolution of the free surface propagated in the presence ((---) Free Surface, (—) Envelope) and in the absence of vorticity ((---) Free Surface, (—) Envelope). (b): Maximum value of the envelope plotted as a function of the maximum value of the vorticity, for several values of the background current velocity.

In the meantime, the green and magenta lines correspond to water waves propagating in the presence of the current field obtained with the parameters $U = -0.2m \cdot s^{-1}$ and $S_0 = -0.2s^{-1}$. This new parameters provide a spatial distribution of $U_0(x)$ and $S(x)$ of Gaussian shape. Here again, the green line correspond to elevation, while the magenta corresponds to the related envelope.

It is interesting to notice how the interaction due to the vorticity is important. Indeed, in the case considered here, the maximum reached by the envelope is increased by 50% when vorticity is present. At the end of the numerical tank, the vorticity vanishes, accordingly to the Gaussian distribution considered in Eq. (49). The amplitude of water waves decreases, and becomes very similar to its value before encountering the modified area. Simultaneously, an important phase modification is observed. The phase shift between water waves propagated in the absence of vorticity, and water waves which encountered variations of the vorticity is close to $3\pi/4$.

The subplot (b) in Fig. 3 illustrates the influence of vorticity on the envelope maximum. Indeed, these curves represent the maximum value of the envelope along the wave tank, E_{max} , plotted as a function of the value of vorticity parameter S_0 considered. The four curves correspond to four values of the parameter U considered. Thus, this curve can be interpreted as the normalized amplification of water waves due to the presence of vorticity. From this figure, it appears that vorticity can have significant influence, since the water waves amplification can reach, in some specific cases, a factor three. Furthermore, it appears that negative vorticities have a stronger influence on the envelope dynamics than positive ones.

4.2.2. Wave scattering by sinusoidal bathymetry in the presence of current

The second case considered here is designed to emphasize the evolution of water waves in the presence of a slowly varying vorticity field, when bathymetry variations are considered. A classical two dimensional case corresponds to the Bragg reflection. Furthermore, in this subsection, we take advantage of existing experimental results.

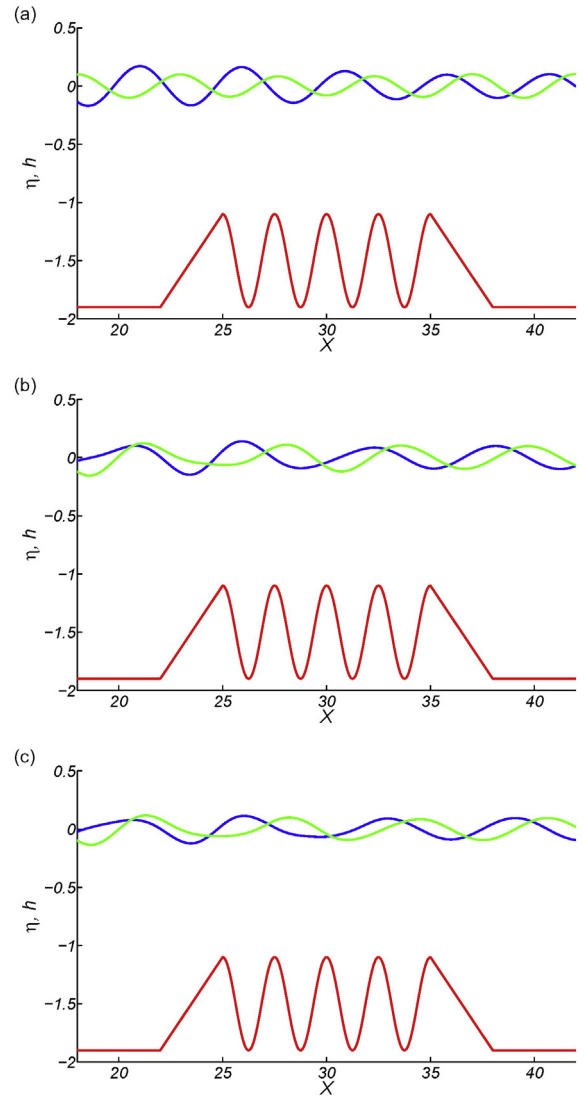


Fig. 4. Free surface elevation (real part (—) and imaginary part (---)) as calculated by the present model in the case of waves of period $T = 2.5s$ propagating over the rippled bed. (a) no current, (b) homogeneous current $U_0 = 0.4m \cdot s^{-1}$, (c) vertically sheared current $U_0 = 0.4m \cdot s^{-1}$, $S = 0.2s^{-1}$.

Indeed, a case of wave scattering over a sinusoidal bottom in the presence of following current was investigated by Magne et al. (2005). Waves were generated in a flume with and without current and propagated over a patch of four sinusoidal bars before dissipating on a beach. The mean depth over the sinusoidal patch is $h = 1.5m$ and the base depth $1.9m$. The amplitude of the bars is $0.4m$ with a horizontal bottom wavelength of $\lambda_0 = 2.5m$. The sinusoidal patch is $10m$ long including four bottom periodic cells, and is extended by $3m$ -long adapter ramps at the beginning and at the end, to allow for a smooth transition. The above bottom profile is illustrated in Fig. 4, along with the calculated free-surface elevation corresponding to a harmonic incident waves of period $T = 2.5s$, as calculated by the present model. In particular three cases have been examined: (a) waves without current, (b) waves with a homogeneous following current $U_0 = 0.4m \cdot s^{-1}$, and (c) same as before but with a vertically sheared current, where the shear is also horizontally constant $S = 0.2s^{-1}$.

A comparison of the present method results vs. experimental measurements for the reflection coefficient (from Magne et al., 2005) is presented in Fig. 5, for waves without current (shown by the blue line) and with a horizontal current flowing in the positive x-direction with velocity $U_0 = 0.4m \cdot s^{-1}$ (shown by the green line) and the shear current

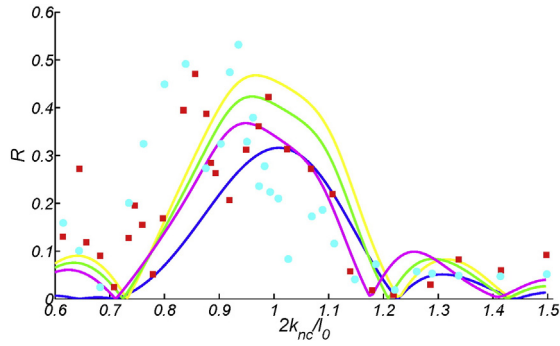


Fig. 5. Reflection coefficient vs. normalized resonant wave number in the case of sinusoidal bottom profile. Present method results are shown by using thick solid lines ((—)) $U_0=0m.s^{-1}$ & $S=0s^{-1}$, (—) $U_0=0.4m.s^{-1}$ & $S=0s^{-1}$, (—) $U_0=0.4m.s^{-1}$ & $S=-0.2s^{-1}$, and (—) $U_0=0.4m.s^{-1}$ & $S=0.2s^{-1}$. Experimental data from Magne et al. (2005) are shown using squares (■, $U_0=0m.s^{-1}$) and bullets (●, $U_0=0.4s^{-1}$), respectively.

(shown by the yellow and magenta lines). Results are presented as a function of the normalized resonant wave number $2k_{nc}/l_0$, where $l_0 = 2\pi/\lambda_0$, and where k_{nc} is the wave number corresponding to the base water depth $h = 1.9m$ for a gravity wave of angular frequency ω without current, so that $\omega = \sqrt{gk_{nc} \tanh(k_{nc}h)}$.

When analysing these results, several remarks occur. First, when considering only numerical results, the influence of vorticity on Bragg resonance appears. Indeed, the solid blue line corresponds to the results involving no current, the green line is the case $U_0 = 0.4m.s^{-1}$ and $S = 0s^{-1}$, the yellow line corresponds to the case $U_0 = 0.4m.s^{-1}$ and $S = -0.2s^{-1}$, while the magenta line is the case $U_0 = 0.4m.s^{-1}$ and $S = 0.2s^{-1}$. The comparison between the blue and green line illustrate the influence of the current on Bragg reflection coefficient. It is interesting to notice that the maximum value of this coefficient varies from $R = 0.3$ to $R = 0.45$ when strong current is present. This result, however, was already known. The novelty here comes when considering the vorticity. The reflection coefficient, in the latter case, may vary between values ranging from $R = 0.35$ to $R = 0.5$. The maximum location is also found to be slightly affected.

Considering the comparison of the present results against the experimental data, it is observed that the inclusion of current provides better agreement of model predictions with measured values of the reflection coefficient. Moreover, the inclusion of shear in the current has an effect to further increase the peak value of the reflection coefficient. Future research will focus on the investigation of this finding by experiments in wave flume with controllable sheared current.

4.3. Two dimensional propagation

The simulations presented here are designed to emphasize the importance of vorticity on water wave's propagation when two dimensional effects are considered. To do so, we consider the case of waves scattering over a linear bottom profile, taking into account the effects of an opposing jet-like flow modelling a rip current. Wave-induced rip currents are due to the three dimensional circulation induced by wave forcing. Indeed, the longshore flow fields converge into periodic rips and form independent circulation cells in the inshore region, which plays an important role in coastal morphodynamics. These currents, in conjunction with local amplification of wave energy, are responsible for many accidents near beaches.

In several works concerning the structure of rip currents, based both on experimental studies, as e.g., Haller et al. (1997); Haas and Svendsen (2002), and observations MacMahan et al. (2005), it is reported that most of the shear in rip current flows is contained in the crest-trough region indicating a mostly constant vertical velocity profile, from the bottom up to the wave trough. The treatment of wave scattering by current

profiles characterized by different vertical slopes in various parts necessitates significant modification, and such an extension is left to be examined in future work. On the other hand, in the detailed laboratory study of rip channel flow by Haas and Svendsen (2002) it is clearly shown that, although there is little variation of the vertical profile inside the channel, still linear variation is quite evident, especially moving in the offshore direction, where the current velocity diminishes at the bottom or even becomes shoreward at some offshore locations; see, e.g., Fig. 12 in Haas and Svendsen (2002). In conclusion, with the exception of the crest-trough region, rip currents could present a strong depth variation outside the breakers and little depth variation inside the channel or the convergence zone, that can be modelled by considering the present single linear model, Eq. (1).

In order to illustrate the combined effects of shear in rip flow and bathymetry into the wave pattern, in this section we examine a beach of uniform slope 1:50 similar to the one considered by Liu (1983). This example has been further studied by many authors (see e.g. Chen et al., 2005; Liau et al., 2011; Belibassakis et al., 2014). Chen et al. (2005) describe the structure of the rip current $U = (U_0, V_0)$ considered in this example by means of the relations

$$U_0 = -0.1442sF\left(\frac{s}{76.2}\right)F\left(\frac{y}{7.62}\right)$$

$$V_0 = -0.5192\left(2 - \left(\frac{s}{76.2}\right)^2\right)F\left(\frac{s}{76.2}\right)\int_0^{y/7.62} F(\tau)d\tau, \quad (51)$$

where lengths are in m and velocities in m/s , and where $s = x - 300m$ is the distance from the shore. Furthermore, F refers to the function defined as

$$F(\tau) = \frac{1}{\sqrt{2\pi}} \exp\left(-\frac{\tau^2}{2}\right). \quad (52)$$

In this work, we consider two distinct cases. First, the case studied by these authors is reproduced for sake of validation of the numerical scheme. The current described by Eq. (51) is considered to be uniform with depth, and to vary slowly within the numerical domain, as presented in Fig. 6, and its maximum value is $1.06m/s$. Then, a second case is considered, involving vorticity. Here, the current described by Eq. (51) is not considered to be uniform anymore, but to vary with depth. Based on the above remarks, we select as an indicative value of the shearing coefficient

$$S(x, y) = \frac{U(x, y)}{h(x, y)}, \quad \text{for } x \leq 300m, \quad (53)$$

i.e. outside and offshore the convergence zone, so that the current velocity field becomes zero at the bottom in this subregion.

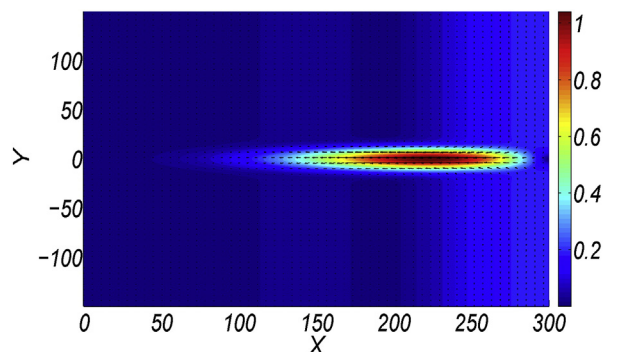


Fig. 6. Distribution of the surface current within the numerical domain.

Furthermore, we select the shear to vanish

$$S(x, y) = 0, \text{ for } x > 300m, \quad (54)$$

in the convergence zone and moving to the onshore subregion.

In both cases, we consider unit-amplitude harmonic waves of period $T = 8s$ propagating along the x -axis, normally to the bottom contours. A subdomain of constant depth $h = 4m$ has been assumed in subregion $x \leq 100m$ in order to specify the incident wave conditions. Furthermore, a cut-off value of depth equal to $h = 0.04m$ has been used in order to numerically treat the zero-depth singularity at the shore-line $x = 300m$, and further ($x \geq 300m$). Thus, the numerical domain considered was $350m$ by $350m$, discretised by means of 501 equidistant points along each horizontal direction, which are enough for numerical convergence. Boundary conditions used here are those described in Section 4.1.

Results of these simulations are displayed in Figs. 7 and 8. In Fig. 7, normalized wave amplitude (a) and phase (b) are presented when no vorticity is involved within the numerical simulation. In the lower part of this figure, normalized amplitude (c) and phase (d) are also displayed, but when the vorticity field is considered. Qualitative behaviour observed in Belibassakis et al. (2014) is very well reproduced, including the wave focusing over the rip current, and the phase shift induced when approaching the coast line. When vorticity is considered, the behaviour observed is different. Although the distribution of wave amplitudes remains similar, the difference concerning the wave phase is much more striking. Indeed, the phase shift observed around $(x, y) = (250, 0)$ is not present in the latter case.

Focusing on wave amplitude, comparisons are presented in Fig. 8. More specifically, Fig. 8(a) displays the evolution of the normalized wave amplitude along the centreline of the numerical domain ($y = 0$),

and presents the results obtained by several authors in the absence of vorticity. Results given by Liu (1983) are shown by using magenta diamonds, results obtained by Chen et al. (2005) are indicated by yellow squares, results given by Liau et al. (2011) are displayed by cyan circles, while results obtained by Belibassakis et al. (2014) correspond to the green solid line. For sake of comparison, the present results, when no vorticity is considered, are given by the solid blue line, and present a very good agreement with former works. In the meantime, the solid red line corresponds to the results obtained with this method, when the shear is taken into account. From this figure, a confirmation of the qualitative behaviour observed in Fig. 7 is found. The wave normalized amplitude, along the centreline of the numerical domain, is not significantly affected by the presence of vorticity. This is probably explained by the symmetry of the problem at hand.

On the other hand, the phase difference due to the presence of vorticity observed in Fig. 7 must have a significant impact on local properties of wave amplitudes. These differences can be seen in Fig. 8(b). Indeed, the normalized wave amplitudes along the shore ($x = 250m$) are plotted for both cases. The solid blue line corresponds to the solution obtained in the absence of vorticity, while the solid red line is the solution when vorticity is present. From this figure, it appears that if the maximum of the normalized amplitude on the axis are not significantly changed, they present important differences on both parts of the rip current. Indeed, calm zones are observed on both sides of the rip current in the absence of vorticity. These zones are not reproduced when vorticity is considered. This observation emphasizes the effect of vorticity difference on the local wave properties. Indeed, if the global energy focused on the axis of symmetry remains similar in both cases, its origin is rather different from one case to another. This observation emphasizes the strong role played by vorticity on the local properties of the wave field in two dimensional cases of propagation.

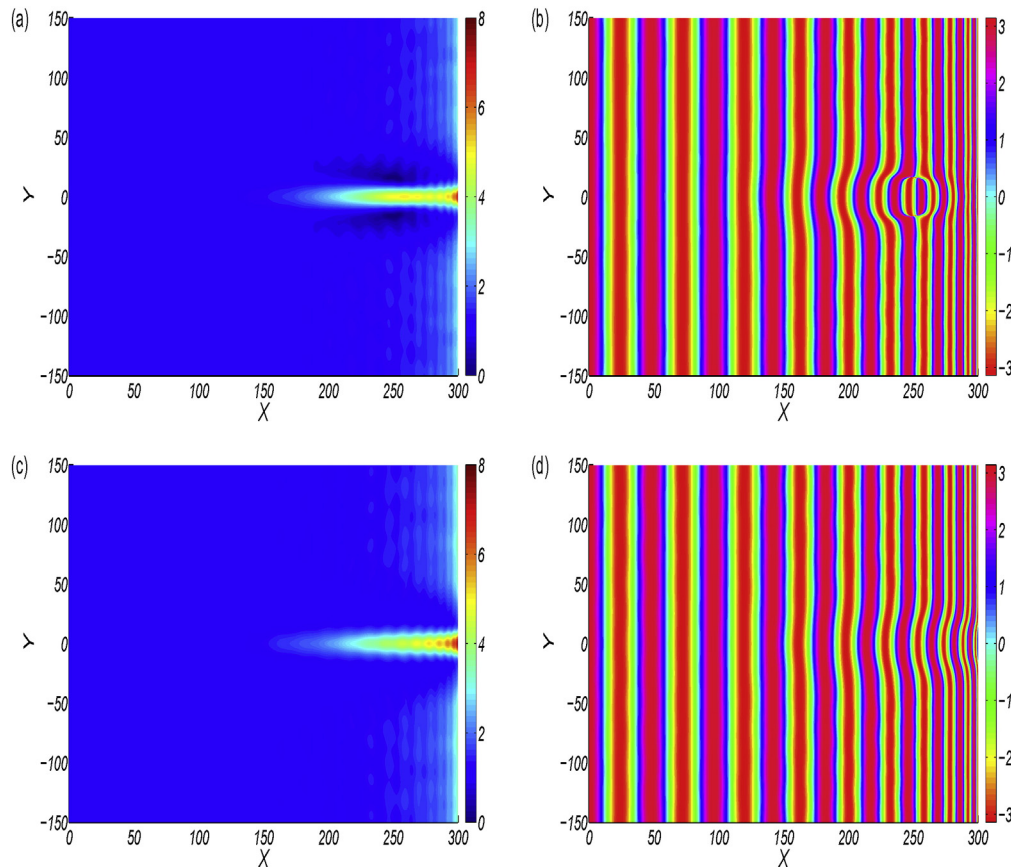


Fig. 7. (a): Normalized wave amplitude within the numerical domain in the absence of vorticity. (b): Normalized wave phase within the numerical domain in the absence of vorticity. (c): Normalized wave amplitude within the numerical domain in the presence of vorticity. (d): Normalized wave phase within the numerical domain in the presence of vorticity.

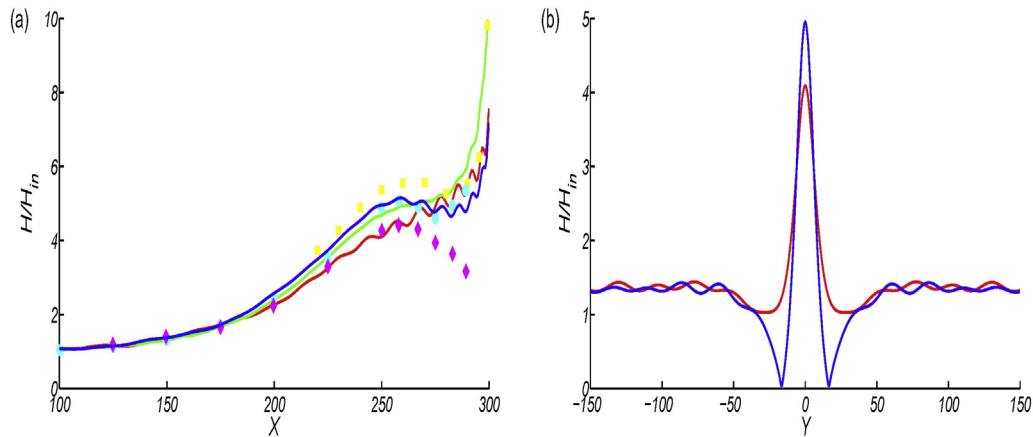


Fig. 8. (a): Normalized wave amplitude along the centreline ($y=0$). Former results by Liu (1983) (\blacklozenge), Chen et al. (2005) (\blacksquare), Liao et al. (2011) (\bullet), Belibassakis et al. (2014) (\blacktriangle) are plotted together with the present simulations obtained in the absence of vorticity (—). Results obtained in the present of vorticity are also displayed, for sake of comparison (—). (b): Normalized wave amplitude along the shoreline ($x=250m$). Results obtained in the absence of vorticity (—) are plotted together with results obtained when vorticity is considered.

5. Concluding remarks

A new formulation of the mild-slope equation is derived and studied to describe wave scattering by horizontally slowly varying sheared currents and bathymetry. In its present form, this equation provides the dynamics of linear water waves propagating in the presence of inhomogeneous currents characterized by linear vertical profile. The vorticity is assumed to be locally constant, possibly strong. On the other hand, the horizontal variations of the bathymetry, and of the current properties are assumed to be slow with respect to the wavelength. When no horizontal variations are considered, this equation reduces to the classically known free surface equation and dispersion relation. Furthermore, when no vorticity is considered, this equation reduces to classically known mild-slope equation. With the aid of selected examples the effect of shear on the wave pattern and dynamics is illustrated, which could become quite important in specific cases.

The present equation could be extended to more general cases, including higher order terms with respect to the bottom slope (Toledo et al., 2012), or multimodal expansions for the potential (Belibassakis et al., 2011). Future work will also focus on the investigation of the evolution of wave action and wave energy as predicted by the present phase-resolving model, in applications to nearshore and coastal regions. In particular, wave action plays a central role in the development and validation of phase-averaged wave models, and its conservation in the presence of vertical currents is subject to controversy (see e.g. (Bretherton and Garrett, 1969; Voronovich, 1976)).

Acknowledgment

This work was supported by ANR grant N°ANR-13-ASTR-0007. The DGA (Direction Générale de l'Armement, France) is acknowledged for its financial support for the Ph-D thesis of Jenna Charland. Furthermore, anonymous reviewers are acknowledged for their helpful comments to improve the present paper. Finally, the authors would like to thank Pr. Kirby and Dr. Ardhuin for really useful discussions.

References

- Athanassoulis, G.A., Belibassakis, K.A., 1999. A consistent coupled-mode theory for the propagation of small-amplitude water waves over variable bathymetry regions. *J. Fluid Mech.* 389, 275–301.
- Bateman, H., 1929. Notes on a differential equation which occurs in the two-dimensional motion of a compressible fluid and the associated variational problems. *Proc. R. Soc. Lond. A* 125, 598–618.
- Belibassakis, K.A., 2007. A coupled-mode model for the scattering of water waves by shearing currents in variable bathymetry. *J. Fluid Mech.* 578, 413–434.

- Belibassakis, K.A., Gerostathis, T.P., Athanassoulis, G.A., 2011. A coupled-mode model for water wave scattering by horizontal, non-homogeneous current in general bottom topography. *Appl. Ocean Res.* 33, 384–397.
- Belibassakis, K.A., Athanassoulis, G.A., Gerostathis, T.P., 2014. Directional wave spectrum transformation in the presence of strong depth and current inhomogeneities by means of coupled-mode model. *Ocean Eng.* 87, 84–96.
- Berkhoff, J.C.W., 1976. *Mathematical Models for Simple Harmonic Linear Water Waves. Wave Diffraction and Refraction.* De Voorst Laboratory of the Delft Hydraulics Laboratory (PhD thesis).
- Booij, N., 1981. *Gravity Waves on Water with Non-Uniform Depth and Current (PhD thesis)* Delft University of Technology, The Netherlands.
- Bretherton, F.P., Garrett, C.J.R., 1969. Wavetrains in inhomogeneous moving media. *Proc. R. Soc. A* 302, 529–554.
- Chamberlain, P.G., Porter, D., 1995. The modified mild-slope equation. *J. Fluid Mech.* 291, 393–407.
- Chen, W., Panchang, V., Demirebilek, Z., 2005. On the modeling of wave-current interaction using the elliptic mild-slope wave equation. *Ocean Eng.* 32, 2135–2164.
- Constantin, A., 2011. Two-dimensionality of gravity water flows of constant nonzero vorticity beneath a surface wave train. *Eur. J. Mech. B. Fluids* 30, 12–16.
- Constantin, A., Varvaruca, E., 2011. Steady periodic water waves with constant vorticity: regularity and local bifurcations. *Arch. Ration. Mech. Anal.* 199, 33–67.
- Dalrymple, R.A., 1974. A finite amplitude wave on linear shear current. *J. Geophys. Res.* 79 (30).
- Dean, R.G., Dalrymple, R.A., 1991. *Water Wave Mechanics for Engineers and Scientists* vol. 2. Word Scientific.
- Greenwood, B., Osborne, P.D., 1990. Vertical and horizontal structure in cross-shore flows: an example of undertow and wave set-up on a barred beach. *Coast. Eng.* 14 (6), 543–580.
- Haas, K.A., Svendsen, I.A., 2002. Laboratory measurements of the vertical structure of rip currents. *J. Geophys. Res.* C5, 3047.
- Haller, M.C., Dalrymple, R.A., Svendsen, I.A., 1997. *Rip Channels and Nearshore Circulation. Proceedings of the International Conference on Coastal Research through Large Scale Experiments, Plymouth, UK.*
- Jonsson, I.G., 1990. Wave-Current Interactions. In: LeMehaute, B., Hanes, D.M. (Eds.), *The Sea* vol. 9. John Wiley, New York, pp. 65–120.
- Jonsson, I.G., Brink-Kjaer, O., Thomas, G.P., 1978. Wave action and set down for waves on a shear current. *J. Fluid Mech.* 87 (3), 401–416.
- Kirby, J.T., 1984. A note on linear surface wave-current interaction over slowly varying topography. *J. Geophys. Res.* 89 (C1), 745–747 (January 20).
- Kirby, J.T., 1989. A note on parabolic radiation boundary conditions for elliptic wave calculations. *Coast. Eng.* 13, 211–218.
- Kirby, J.T., Chen, T., 1989. Surface waves on vertically sheared flows: approximate dispersion relations. *J. Geophys. Res.* 94 (C1), 1013–1027.
- Kirby, J.T., Dalrymple, R.A., 1983. Propagation of obliquely incident water waves over a trench. *J. Fluid Mech.* 133, 47–63.
- Lavrenov, I.V., Porubov, A.V., 2006. Three reasons for freak wave generation in the non-uniform current. *Eur. J. Mech. B. Fluids* 25, 574–585.
- Liao, J.M., Roland, A., Hsu, T.W., Ou, S.H., Li, Y.T., 2011. Wave refraction-diffraction effect in the wind wave model wwm. *Coast. Eng.* 58, 429–443.
- Liu, P.L.F., 1983. Wave-current interactions on a slowly varying topography. *J. Geophys. Res.* 88 (C7), 4421–4426.
- Liu, Z., Lin, Z., Liao, S., 2014. Phase velocity effects of the wave interaction with exponentially sheared current. *Wave Motion* 51, 967–985.
- Longuet-Higgins, M.S., 1983. On integrals and invariants for inviscid, irrotational flow under gravity. *J. Fluid Mech.* 134, 155–159.
- Longuet-Higgins, M.S., Stewart, R.W., 1961. The changes in amplitude of short gravity waves on steady non-uniform currents. *J. Fluid Mech.* 10 (4), 529–549.
- Luke, J.C., 1967. A variational principle for a fluid with a free surface. *J. Fluid Mech.* 27 (part 2), 395–397.

- MacMahan, J.H., Thornton, E.B., Stanton, T.P., Reniers, A.J.H.M., 2005. Ripex: observations of a rip current system. *Mar. Geol.* 218, 113–134.
- Magne, R., Rey, V., Arduin, F., 2005. Measurement of wave scattering by topography in the presence of currents. *Phys. Fluids* 17, 126601.
- Massel, S.R., 1993. Extended refraction–diffraction equation for surface waves. *Coast. Eng.* 97–126.
- Mei, C.C., 1994. *The Applied Dynamics of Ocean Surface Waves* vol. 1. World Scientific Publishing (second reprint ed.).
- Nwogu, O.G., 2009. Interaction of finite-amplitude waves with vertically sheared current fields. *J. Fluid Mech.* 627, 179–213.
- Panchang, V., Pearce, B.R., Wei, G., Cushman-Roisin, B., 1991. Solution of the mild-slope wave problem by iteration. *Appl. Ocean Res.* 13, 187–199.
- Peregrine, D.H., 1976. Interactions of water waves and currents. *Adv. Appl. Mech.* 16, 9–117.
- Putrevu, U., Svendsen, I.A., 1993. Vertical structure of the undertow outside the surf zone. *J. Geophys. Res.* C12, 22707–22716.
- Radder, A.C., 1979. On the parabolic equation method for water-wave propagation. *J. Fluid Mech. (part 1)*, 159–176.
- Rey, V., 1992. Propagation and local behavior of normally incident gravity waves over varying topography. *Eur. J. Mech. B. Fluids* 11 (2), 213–232.
- Rey, V., Touboul, J., Guinot, F., 2012. Large Scale Experimental Study of Wave Current Interactions in Presence of a 3d Bathymetry. Proceedings of the 14th International Congress of International Maritime Association of the Maritime (IMAM). CRC Press, London, pp. 873–880.
- Rey, V., Charland, J., Touboul, J., 2014. Wave – current interaction in the presence of a 3d bathymetry: deep water wave focusing in opposite current conditions. *Phys. Fluids* 26, 096601.
- Seliger, R.L., Whitham, G.B., 1968. Variational principles in continuum mechanics. *Proc. R. Soc. Lond. A* 305, 1–25.
- Shrira, V.I., 1993. Surface waves on shear currents: solution of the boundary value problem. *J. Fluid Mech.* 252, 565–584.
- Simmen, J.A., 1984. Steady Deep-Water Waves on a Linear Shear Current (PhD thesis) California Institute of Technology, Pasadena, California.
- Simmen, J.A., Saffman, P.G., 1985. Steady deep-water waves on a linear shear current. *Stud. Appl. Math.* 73, 35–57.
- Skop, R.A., 1987a. An approach to the analysis of the interaction of surface waves with depth-varying current fields. *Appl. Math. Model.* 11.
- Skop, R.A., 1987b. An approximate dispersion relation for wave–current interactions. *J. Waterw. Port C-ASCE* 113, 187–195.
- Smith, R., 1976. Giant waves. *J. Fluid Mech.* 77, 417–431.
- Son, S., Lynett, P., 2014. Interaction of dispersive water waves with weakly sheared currents of arbitrary profile. *Coast. Eng.* 90, 64–84.
- Soulsby, R.L., 1990. *Tidal Current Boundary Layers*, Volume 9(a) of *Ocean Eng. Sc.* John Wiley, New York, USA, pp. 523–566.
- Stepanyants, Y.A., Yakubovich, E.I., 2011. Scalar description of three-dimensional vortex flows of an incompressible fluid. *Dokl. Akad. Nauk* 436 (6), 764–767.
- Stewart, R.H., Joy, J.W., 1974. Hf radio measurements of surface currents. *Deep-Sea Res.* 21, 1039–1049.
- Swan, C., 1990. An Experimental Study of Wave on a strongly Sheared Current Profile. *Coastal Engineering Proc.* vol. 1 (22), pp. 489–502.
- Swan, C., Cummins, I.P., James, R.L., 2001. An experimental study of two-dimensional surface water waves propagating on depth varying currents. *J. Fluid Mech.* 428, 273–304.
- Teles Da Silva, A.F., Peregrine, D.H., 1988. Steep, steady surface waves on water of finite depth with constant vorticity. *J. Fluid Mech.* 195, 281–302.
- Thomas, G.P., 1990. Wave–current interactions: an experimental and numerical study. Part 1. Nonlinear waves. *J. Fluid Mech.* 216, 505–536.
- Thomas, G.P., Klopman, G., 1997. Wave?Current Interaction in the Nearshore Region. In: Hunt, J.N. (Ed.), *Gravity Waves in Water of Finite Depth*. Computational Mechanics Publications.
- Thompson, P.D., 1949. The propagation of small surface disturbances through rotational flow. *Ann. N. Y. Acad. Sci.* 51, 463–474.
- Toledo, Y., Agnon, Y., 2011. Three dimensional application of the complementary mild-slope equation. *Coast. Eng.* 58, 1–8.
- Toledo, Y., Hsu, T.-W., Roland, A., 2012. Extended time dependent mild-slope and wave action equations for wave–bottom and wave–current interactions. *Proc. R. Soc. A* 468, 184–205.
- Voronovich, A., 1976. The propagation of surface and internal waves in an approach of geometrical optics. *Izv. USSR Acad. Sci. Phys. Atmos. Oceans* 12 (8), 850–857.
- Wahlen, E., 2009. Steady water waves with a critical layer. *J. Differ. Equ.* 246, 2468–2483.
- Whitham, G.B., 1974. *Linear and Nonlinear Waves*. John Wiley & Sons, New York.